

Magnetic structure and fluctuations of Gd₂IrIn₈: A resonant x-ray diffraction study

E. Granado,^{1,*} P. G. Pagliuso,² C. Giles,² R. Lora-Serrano,^{1,2} F. Yokaichiya,² and J. L. Sarrao³
¹Laboratório Nacional de Luz Síncrotron, Caixa Postal 6192, CEP 13084-971 Campinas, São Paulo, Brazil
²Instituto de Física "Gleb Wataghin," UNICAMP, 13083-970 Campinas, São Paulo, Brazil
³Los Alamos National Laboratory, Los Alamos, New Mexico 87545, USA
 (Received 10 November 2003; published 9 April 2004)

Resonant x-ray diffraction measurements on Gd₂IrIn₈ reveal an antiferromagnetic structure below $T_N = 40.8$ K with wave vector $\zeta = (\frac{1}{2}, 0, 0)$ and the Gd moments lying in the tetragonal ab plane, indicating partly frustrated exchange interactions. Strong (over three orders of magnitude) dipolar resonant enhancements of the magnetic reflections were observed at both Gd L_{II} and L_{III} edges, indicating a relatively high magnetic polarization of the Gd $5d$ levels. Three-dimensional magnetic fluctuations are evidenced below T_N , while measurements taken slightly above T_N are consistent with two coexisting length scales for the magnetic correlations. Implications of these results for the physics of Ce_{*n*}M_{*m*}In_{*3n+2m*} ($M = \text{Co, Rh, or Ir}$) heavy-fermion superconductors are discussed.

DOI: 10.1103/PhysRevB.69.144411

PACS number(s): 75.25.+z, 74.70.Tx, 75.40.-s, 75.10.-b

I. INTRODUCTION

The series of intermetallic compounds $R_nM_m\text{In}_{3n+2m}$ ($R = \text{rare earth; } M = \text{Co, Rh, or Ir}$) has recently attracted considerable interest due to the discovery of a new class of heavy-fermion superconductors for some compounds with $R = \text{Ce}$.¹⁻⁴ While the Cooper pairing mechanism remains unknown, most evidence points to antiferromagnetic spin fluctuations.⁵ In order to fully understand the nature of the magnetic interactions in this system and their possible connection with the superconductivity found for $R = \text{Ce}$, it is necessary to investigate the evolution of the magnetic structure as a function of the rare-earth ion R , as well as the dimensionality (n, m).⁶⁻¹⁰

In general terms, the magnetic properties of the series depend on the balance between anisotropic Ruderman-Kittel-Kasuya-Yosida (RKKY) interactions, crystal-field anisotropies, and, for $R = \text{Ce}$, Kondo interactions. While the crystal-field effects are highly dependent on the ground state of each particular rare-earth ion, some aspects of the RKKY interactions, on the other hand, are expected to be much less dependent on R , because they are mediated through spatially extended conduction electrons. In this context, the magnetism of Gd-based compounds is particularly relevant. This is because the $4f$ shell of this ion is half filled with seven electrons, thus being spherically symmetric with null orbital magnetic moment. In this case, the crystal-field anisotropy, as well as any effect arising from the spin-orbit coupling, does not play a dominant role. Therefore, the magnetism shown by Gd-based compounds is a reliable signature of the dominant RKKY interactions, and by extension of the Fermi surface of the system under investigation. Since the neutron nuclear absorption cross section of Gd is prohibitively high, alternative techniques must be employed to understand the microscopic magnetism of Gd-based compounds.

In this work, we investigate the magnetism of bilayer Gd₂IrIn₈ by means of magnetic resonant x-ray diffraction at the Gd L_{II} and L_{III} edges. $((2n+1)/2, k, l)$ magnetic Bragg reflections (n, k , and l integers) were observed below T_N

$= 40.8$ K, corresponding to a commensurate magnetic wave vector $\zeta = (\frac{1}{2}, 0, 0)$. The Gd magnetic moments lie in the tetragonal ab plane. Remarkably, large dipolar enhancements of the magnetic Bragg reflections were observed at the Gd L_{II} and L_{III} edges. Such characteristics suggest a relatively high Gd: $5d$ magnetic polarization in this compound. Another interesting feature of the resonances is the magnetic diffraction anomalous fine structure (DAFS) observed above both studied edges. The T dependence of the magnetic order parameter is typical for a three-dimensional Heisenberg system, with the critical exponent for the sublattice magnetization $\beta = 0.394(4)$. Interestingly, two length scales for the magnetic correlations above T_N are evidenced by our data. Some aspects of the nature and dimensionality of the exchange interactions are discussed from the perspective of our results. Possible implications of this work to the physics of the Ce_{*n*}M_{*m*}In_{*3n+2m*} ($M = \text{Co, Rh, and Ir}$) heavy-fermion superconductors are suggested.

II. EXPERIMENTAL DETAILS

Gd₂IrIn₈ was grown from the melt in In flux as described previously.¹ The unit-cell dimensions and macroscopic properties of this compound are described in Ref. 11. A crystal with dimensions $5 \times 2 \times 0.3$ mm³ was chosen for our study and the $(0, 0, l)$ flat surface was finely polished to yield a mosaic width of $\sim 0.05^\circ$ full width at half maximum.

The x-ray-diffraction measurements were performed on the XRD2 beamline, placed after a dipolar source at the Laboratório Nacional de Luz Síncrotron, Campinas, Brazil.¹² The sample was mounted on the cold finger of a commercial closed-cycle He cryostat with a cylindrical Be window. The cryostat was fixed onto the Eulerian cradle of a commercial $4+2$ circle diffractometer, appropriate for single-crystal x-ray-diffraction studies. The energy of the incident photons was selected by a double-bounce Si(111) monochromator, with water refrigeration in the first crystal, while the second crystal was bent for sagittal focusing. The beam was vertically focused or collimated by a bent Rh-coated mirror

placed before the monochromator, which also provided filtering of high-energy photons (third- and higher-order harmonics). Unless otherwise noted, a vertically focused beam was used in our measurements, delivering, at 7.24 keV, a flux of 3×10^{10} photons/s at 100 mA in a spot of ~ 0.6 mm (vertical) $\times 2.0$ mm (horizontal) at the sample, with an energy resolution of ~ 5 eV. Our experiments were performed in the vertical scattering plane, i.e., perpendicular to the linear polarization of the incident photons. In most measurements, a solid-state detector was used, except in the polarization study, where a scintillation detector was placed after a Ge(111/333) analyzer crystal. At the energy corresponding to the Gd L_{II} edge, the analyzer placed at the Ge(333) reflection selects ($\sigma \rightarrow \sigma'$) scattering from the sample (i.e., scattered photons with the same polarization as the incident photons), while Ge(111) does not significantly discriminate the photon polarization [$(\sigma \rightarrow \sigma') + (\sigma \rightarrow \pi')$ channel].

III. RESULTS AND ANALYSIS

Above ~ 41 K, all the observed Bragg peaks of Gd_2IrIn_8 are consistent with a tetragonal crystal structure (space group $P4/mmm$), without any detectable magnetic contribution. No evidence for symmetry lowering of the crystal structure was found between 10 and 300 K. Specifically, any distortion in the ab plane must satisfy $|a - b| \leq 0.002 \text{ \AA}$.

Below $T_N = 40.8$ K, additional $((2n+1)/2, k, l)$ Bragg reflections ($n, k,$ and l integers) were observed. Such reflections were dramatically enhanced at the Gd L_{II} and L_{III} edges ($E = 7.93$ and 7.24 keV, respectively) due to resonance phenomena (see below). The polarization properties of a selected reflection, $(\frac{1}{2}, 0, 4)$, were investigated at the L_{II} edge. While a strong reflection was observed at the $(\sigma \rightarrow \sigma') + (\sigma \rightarrow \pi')$ channel, no intensity was detected at the $(\sigma \rightarrow \sigma')$ channel, indicating pure $(\sigma \rightarrow \pi')$ scattering. This result indicates that the $((2n+1)/2, k, l)$ reflections are magnetic in origin, with a dipolar resonance at the Gd L_{II} edge.¹³ This is of course in stark contrast with the polarization properties of the (h, k, l) lattice Bragg peaks (h, k, l integers), where comparable intensities at both channels were observed, indicating a purely unrotated polarization as expected for conventional charge scattering. The observation of $((2n+1)/2, k, l)$ magnetic reflections for Gd_2IrIn_8 is consistent with an antiferromagnetic (AFM) structure with wave vector $\zeta = (\frac{1}{2}, 0, 0)$.

For collinear magnetic structures and σ -polarized incident photons, the polarization dependence of the x-ray magnetic scattering assumes a simple form for dipolar resonances,^{13,14} and the intensities of magnetic Bragg peaks are given by $I^M(\tau) \propto [\sum_j \mathbf{m}_j \cdot \mathbf{k}_f \cos(\tau \cdot \mathbf{r}_j)]^2$, where the sum is over the j th resonant ion in the magnetic unit cell, \mathbf{r}_j is the position of such an ion, τ is the reciprocal-lattice vector for the Bragg reflection, \mathbf{m}_j is the magnetic moment at site j , and \mathbf{k}_f is the wave vector of the scattered light. This expression is valid as long as the quadratic term in \mathbf{m}_j on the magnetic scattering amplitude can be neglected.^{13,14} The magnetic structure of Gd_2IrIn_8 was thus resolved by comparing the intensities of $((2n+1)/2, k, l)$ Bragg reflections with those expected as-

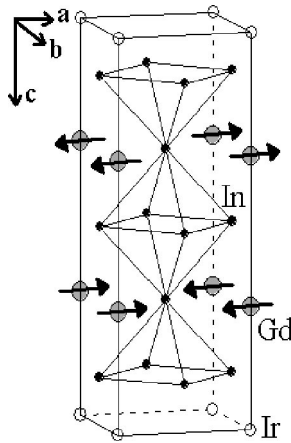
TABLE I. Comparison between observed and calculated intensities of magnetic Bragg reflections, assuming either antiparallel (model I) or parallel (model II) alignment between the moments of the two Gd ions in the same chemical unit cell, normalized by the most intense reflection. Error bars are mostly due to the absorption correction procedure. For model I, calculations assuming the moments \mathbf{m} along each one of the three axes of the tetragonal unit cell are shown. For model II, the calculated intensities do not match the observed ones for any moment direction, and only data with $\mathbf{m} \parallel \mathbf{b}$ are shown. The tetragonal axes \mathbf{a} and \mathbf{b} are defined so that the magnetic wave vector $\zeta \parallel \mathbf{a}$. Experimental data were taken in resonance conditions, at the Gd L_{III} edge.

(h, k, l)	I_{obs}	Model I	Model I	Model I	Model II
		$\mathbf{m} \parallel \mathbf{a}$	$\mathbf{m} \parallel \mathbf{b}$	$\mathbf{m} \parallel \mathbf{c}$	$\mathbf{m} \parallel \mathbf{b}$
$(\frac{1}{2}, 0, 4)$	100	100	100	9	0
$(\frac{1}{2}, 0, 5)$	5(1)	1	1	0	100
$(\frac{1}{2}, 0, 6)$	50(3)	45	41	53	12
$(\frac{1}{2}, 0, 7)$	43(2)	46	40	100	10

suming distinct physical models with collinear Gd magnetic moments, using the expression given above for $I^M(\tau)$.

First of all, we note that the magnetic wave vector $\zeta = (\frac{1}{2}, 0, 0)$ indicates antiparallel ordering of Gd magnetic moments along the \mathbf{a} direction, and parallel moments along \mathbf{b} . Thus, the problem reduces to finding the direction of the magnetic moments, as well as the magnetic coupling along \mathbf{c} , i.e., between the two Gd ions in the same chemical unit cell. Table I shows the observed intensities of a few magnetic Bragg peaks at the Gd L_{III} edge, and a comparison with calculated intensities assuming either parallel or antiparallel coupling along \mathbf{c} , with the moments along either \mathbf{a} , \mathbf{b} , or \mathbf{c} crystallographic directions. The calculated intensities are found to match the observed ones for an AFM coupling between the two Gd ions in the chemical unit cell, and the moments lying in the ab plane. However, a clear distinction of the moment direction in this plane with respect to the magnetic wave vector $\zeta \parallel \mathbf{a}$ could not be made in our experiment (see Table I). The fact that the observed intensities of the $((2n+1)/2, k, l)$ Bragg reflections could be accounted for by a magnetic model further supports the magnetic nature of such peaks. Figure 1 illustrates the Gd magnetic structure of Gd_2IrIn_8 . We should mention that magnetic $(h, (2n+1)/2, l)$ Bragg reflections were also observed, revealing a twinning of the magnetic structure shown in Fig. 1. The intensities of $((2n+1)/2, k, l)$ and $(h, (2n+1)/2, l)$ reflections were not comparable, suggesting large AFM domain sizes, of the order of the beam dimensions ($\sim 1 \text{ mm}^2$).

The resonance properties of the magnetic scattering of Gd_2IrIn_8 were studied at 10 K. Figures 2(a) and 2(b) show the energy dependence of the absorption-corrected intensity of the $(\frac{1}{2}, 0, 4)$ Bragg reflection, around the Gd L_{III} and L_{II} edges, respectively (filled symbols). The energy dependencies of the absorption coefficient $\mu(E)$, obtained from fluorescence emission, are also given as solid lines. Remarkable resonant enhancements of over three orders of magnitude were observed both at the L_{II} and L_{III} edges. To the best of


 FIG. 1. Magnetic structure of Gd_2IrIn_8 .

our knowledge, such strong enhancements are the largest reported in rare-earth L edges. The intensity maximums occur ~ 2 eV above the absorption edges, which were defined as the inflection points of $\mu(E)$. This result is consistent with a dominantly dipolar nature ($2p \rightarrow 5d$) for both resonances. Intensity oscillations of the $(\frac{1}{2}, 0, 4)$ magnetic peak were also observed above the edges, which we ascribe to a magnetic DAFS.¹⁵ Energy-dependent measurements similar to those shown in Figs. 2(a) and 2(b) using a collimated beam with optimum energy resolution ($\delta E \sim 1$ eV) were also taken (not

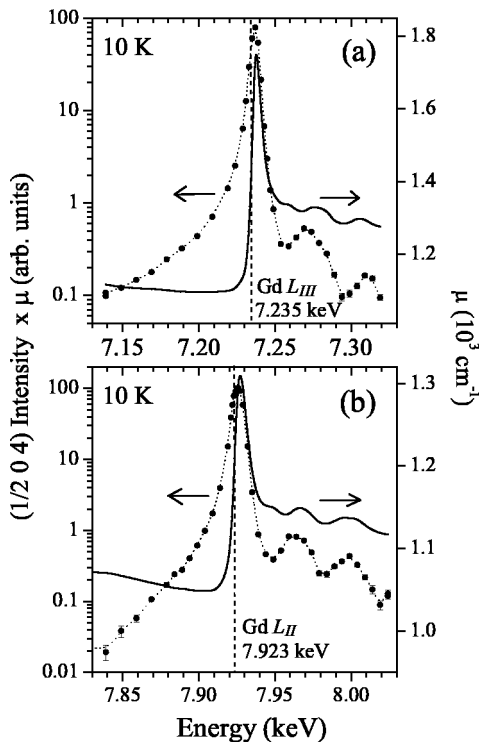


FIG. 2. Energy-dependence of the integrated intensity of the $(\frac{1}{2}, 0, 4)$ Bragg reflection (symbols) across the Gd L_{III} (a) and L_{II} (b) edges. Data were corrected for absorption. Solid lines show the absorption coefficient μ obtained from the fluorescence yield. Vertical dashed lines mark the absorption edges, defined as the inflection points of $\mu(E)$.

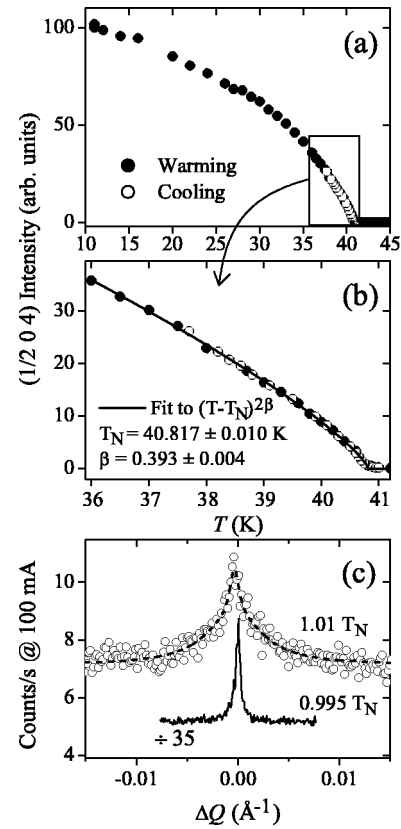


FIG. 3. (a) and (b) Temperature dependence of the magnetic intensity of the $(\frac{1}{2}, 0, 4)$ Bragg reflection, taken on warming (filled circles) and cooling (empty circles). The solid line in (b) is a fit to a power law; the fitting results are also given. (c) Transverse scans of the $(\frac{1}{2}, 0, 4)$ reflection at $0.995T_N$ (solid line, arbitrarily translated in the vertical) and $1.01T_N$ (empty circles). The dashed line is a fit to a broad Lorentzian plus a narrow squared Lorentzian line shape (see Ref. 16). Measurements shown in (a)–(c) were done on resonant conditions at the Gd L_{II} edge ($E = 7.924$ keV).

shown). From the fit of these data to a Lorentzian-squared profile, $I(E) \propto [(E - E_{\text{res}})^2 + (\omega/2)^2]^{-2}$, the resonance widths ω were found to be 7.3(2) and 6.8(2) eV at the L_{II} and L_{III} edges, respectively (corrected for energy resolution).

The temperature dependence of the resonant intensity of the $(\frac{1}{2}, 0, 4)$ magnetic Bragg peak at the L_{II} edge is shown in Figs. 3(a) and 3(b), taken on warming (filled circles) and cooling (open circles). A power-law fit to the data between 36 and 41.2 K yields a critical exponent for the sublattice magnetization $\beta = 0.393(4)$, and a magnetic ordering transition temperature $T_N = 40.817(10)$ K. Errors given in parentheses are statistical only, and represent one standard deviation. This value of T_N is consistent with previous magnetic susceptibility measurements.¹¹ No thermal hysteresis was observed in the magnetic scattering, consistent with a second-order transition. Magnetic critical scattering was also observed at temperatures slightly above T_N . Figure 3(c) shows transverse scans of the $(\frac{1}{2}, 0, 4)$ reflection at $0.995T_N$ (solid line) and $1.01T_N$ (open symbols). Below T_N , the peak width is basically due to the mosaic structure of our crystal, while above T_N the finite magnetic correlation length is clearly the

dominant factor. The peak shape above T_N could not be satisfactorily fitted by a single Lorentzian or squared Lorentzian function (not shown). Interestingly, considerable improvement in the fit was achieved when two components with distinct widths were considered [see dashed line in Fig. 3(c)], consistent with two length scales in the magnetic critical scattering of Gd_2IrIn_8 . This effect seems to be analogous to that observed in a number of materials (see, for example, Refs. 16–19). While it is generally believed that the “broad” component is due to conventional critical fluctuations, the “narrow” component has been attributed to long-ranged correlated quenched disorder in the near surface region.²⁰ A detailed investigation of the temperature dependence of the critical scattering above T_N , which might lead to the critical exponent of the inverse correlation length, ν , is beyond the scope of the present work.

IV. DISCUSSION

The magnetic structure of Gd_2IrIn_8 illustrated in Fig. 1 reveals an interesting ground state for this compound. In fact, the electronic configuration of the Gd $4f$ shell ($S=7/2; L=0$) is uniquely simple among the rare earths, and excludes the possibility of a competition, on the same footing, of RKKY interactions with other terms such as crystal-field anisotropies. Despite this apparent simplicity, the Gd moments are parallel along one Gd-Gd nearest-neighbor direction (\mathbf{a} axis), and antiparallel along the other two. Perhaps more intriguing is the fact that the magnetic unit cell does not show the same tetragonal symmetry as the chemical one, being doubled along a particular tetragonal direction. These characteristics are equivalent to those found in the magnetic structure of NdRhIn_5 .¹⁰ It is therefore apparent that the first-neighbor Gd-Gd magnetic interaction does not determine the magnetic structure of the title compound. Since RKKY interactions are dominant for Gd-based compounds, the nontrivial magnetic ground state of Gd_2IrIn_8 must be directly related to the Fermi surface of this material. As already mentioned, some aspects of the Fermi surface of Gd-based compounds may be generalized to other members of the $R_nM_m\text{In}_{3n+2m}$ (R =rare earth; M =Co, Rh, or Ir) family, and may be relevant for a deeper understanding of the (presumably) magnetically driven heavy-fermion superconductivity of the Ce-based compounds.

Although it is clear that a detailed theoretical analysis is necessary to fully understand the magnetic structure of Gd_2IrIn_8 , some insight is gained with a few simple considerations. First, the relatively large Gd-Gd first-nearest-neighbor distance (~ 4.6 Å) indicates that the exchange interactions between Gd $4f$ electrons are mediated through conduction electrons with significant In $5p$ character, leading to Gd-In-Gd exchange paths. Considering the magnetic network formed by Gd ions at the vertices and In ions at the faces of a cube (GdIn_3 blocks, see Fig. 1), it is evident that the magnetic coupling among Gd ions along the cube edges (first Gd neighbors) and along the face diagonals (second Gd neighbors) must be treated on the same footing, since both interactions involve a Gd-In-Gd exchange path. Indeed, we argue that the magnetic structure of Gd_2IrIn_8 may be under-

stood assuming that Gd-In-Gd exchange integrals along both the cube edges and the face diagonals have comparable magnitudes and the same AFM sign. In this case, inspection of Fig. 1 shows that each Gd spin interacts, on equal footing, with 13 Gd neighbors (five first neighbors along the cube edges and eight second neighbors along the face diagonals). For AFM coupling, it is easily seen that no long-range magnetic structure can simultaneously satisfy all these interactions. Thus, the magnetism in this system is at least partly frustrated. Interestingly, according to this scenario, the most favorable collinear magnetic structure is the one actually realized for Gd_2IrIn_8 (see Fig. 1), with a given Gd moment showing antiferromagnetic alignment with nine (first or second) Gd neighbors, and only four frustrated Gd-Gd interactions with ferromagnetic alignment. The fact that $T_N = 40.8$ K is significantly lower than the paramagnetic Curie-Weiss temperature for Gd_2IrIn_8 ($\theta_p = -75$ K) (Ref. 11) is consistent with the above scenario with partly frustrated exchange interactions.

The distinct magnetic structures of Ce_2RhIn_8 (Ref. 8) and Gd_2IrIn_8 highlight the additional physics necessary to understand the former (and other Ce-based compounds of this family), possibly related with competition among RKKY interactions, the Kondo effect and crystal-field anisotropies. We emphasize that insight on the interplay between exchange and crystal-field anisotropies in this system may be gained by a detailed investigation of the evolution of the magnetic properties (including spin structure) as a function of the rare-earth ion and dimensionality.¹¹ In any case, the partial frustration of the exchange interactions revealed in this work seems to be an important ingredient that pushes the Ce-based compounds close to the quantum criticality that presumably favors the formation of a superconducting state.^{21,22}

The resonance properties of the magnetic Bragg peaks of Gd_2IrIn_8 are also of interest. In fact, the remarkable three orders of magnitude enhancement at both Gd L_{II} and L_{III} edges, due to dipolar ($2p \rightarrow 5d$) resonances (see Fig. 2), indicates a relatively high magnetic polarization of electronic levels with significant Gd $5d$ character. This effect may be due to hybridization of Gd $5d$ levels with the magnetic $4f$ electrons of neighboring Gd sites, via In $5p$. Alternatively, on-site Gd $4f$ - $5d$ hybridization is also possible, since the Gd site is noncentrosymmetric in Gd_2IrIn_8 (see Fig. 1). The relatively high magnetic polarization of rare-earth $5d$ levels is possibly also realized in other members of this family.

The dimensionality of the magnetic fluctuations in this family of compounds is an important element in understanding the origin of the superconducting pairing mechanism in $\text{Ce}_nM_m\text{In}_{3n+2m}$ (M =Co, Rh, and Ir), and to guide the search for new superconducting heavy-fermion compounds with higher critical temperatures. The temperature dependence of the magnetic order parameter in Gd_2IrIn_8 [see Figs. 3(a) and 3(b)] is consistent with three-dimensional fluctuations in the ordered phase, with a relatively high value of the critical exponent $\beta=0.393(4)$. The evolution of this exponent with the dimensionality of the chemical unit cell (cubic \rightarrow bilayer \rightarrow single layer) is presently being investigated, and will be described in a subsequent paper. Perhaps even

more relevant to the context of heavy-fermion superconductivity of the Ce compounds is the nature of the antiferromagnetic correlations in the disordered phase. Interestingly, our measurements taken slightly above T_N [see Fig. 3(c)] are consistent with two coexisting length scales in the magnetic critical scattering of Gd_2IrIn_8 . In view of the apparent generality of this effect,^{14,17-19} we speculate that magnetic correlations of different length scales might also be present in the paramagnetic, and perhaps even in the superconducting state of the Ce-based compounds. Although the magnetic correlations in CeRhIn_5 were already investigated by neutron

scattering,²³ further studies with high resolution in Q space may be necessary to confirm or dismiss this hypothesis.

ACKNOWLEDGMENTS

We thank S.W. Kycia and H. Westfahl, Jr., for helpful discussions, and G. Kellermann for instrumental help. Work at Campinas was supported by FAPESP, CNPq, and ABTLuS. Work at Los Alamos was performed under the auspices of the U.S. Department of Energy.

*Electronic address: granado@lnls.br

¹H. Hegger, C. Petrovic, E.G. Moshopoulou, M.F. Hundley, J.L. Sarrao, Z. Fisk, and J. D. Thompson, Phys. Rev. Lett. **84**, 4986 (2000).

²C. Petrovic, P.G. Pagliuso, M.F. Hundley, R. Movshovich, J.L. Sarrao, J.D. Thompson, Z. Fisk, and P. Monthoux, J. Phys.: Condens. Matter **13**, L337 (2001).

³C. Petrovic, R. Movshovich, M. Jaime, P.G. Pagliuso, M.F. Hundley, J.L. Sarrao, Z. Fisk, and J.D. Thompson, Europhys. Lett. **53**, 254 (2001).

⁴J.D. Thompson, R. Movshovich, Z. Fisk, F. Bouquet, N.J. Curro, R.A. Fisher, P.C. Hammel, H. Hegger, M.F. Hundley, M. Jaime, P.G. Pagliuso, C. Petrovic, N.E. Phillips, and J.L. Sarrao, J. Magn. Magn. Mater. **226**, 5 (2001).

⁵J.D. Thompson, M. Nicklas, A. Bianchi, R. Movshovich, A. Llobet, W. Bao, A. Malinowski, M.F. Hundley, N.O. Moreno, P.G. Pagliuso, J.L. Sarrao, S. Nakatsuji, Z. Fisk, R. Borth, E. Lengyel, N. Oeschler, G. Sparn, and F. Steglich, Physica B **329-333**, 446 (2003).

⁶P.G. Pagliuso, J.D. Thompson, M.F. Hundley, and J.L. Sarrao, Phys. Rev. B **62**, 12 266 (2000).

⁷W. Bao, P.G. Pagliuso, J.L. Sarrao, J.D. Thompson, Z. Fisk, J.W. Lynn, and R.W. Erwin, Phys. Rev. B **62**, R14 621 (2000); **63**, 219901(E) (2001); **67**, 099903(E) (2003).

⁸W. Bao, P.G. Pagliuso, J.L. Sarrao, J.D. Thompson, Z. Fisk, and J.W. Lynn, Phys. Rev. B **64**, 020401 (2001).

⁹M. Amara, R.M. Galéra, P. Morin, T. Veres, and P. Burlet, J. Magn. Magn. Mater. **130**, 127 (1994); M. Amara, R.M. Galéra, P. Morin, J. Voiron, and P. Burlet, *ibid.* **131**, 402 (1994).

¹⁰S. Chang, P.G. Pagliuso, W. Bao, J.S. Gardner, I.P. Swainson, J.L. Sarrao, and H. Nakotte, Phys. Rev. B **66**, 132417 (2002).

¹¹P.G. Pagliuso, J.D. Thompson, M.F. Hundley, J.L. Sarrao, and Z. Fisk, Phys. Rev. B **63**, 054426 (2001).

¹²C. Giles, F. Yokaichiya, S.W. Kycia, L.C. Sampaio, D.C. Ardiles-Saravia, M.K.K. Franco, and R.T. Neuenschwander, J. Synchrotron Radiat. **10**, 430 (2003).

¹³J.P. Hill and D.F. McMorrow, Acta Crystallogr., Sect. A: Found Crystallogr. **52**, 236 (1996).

¹⁴S.W. Lovesey and S.P. Collings, *X-Ray Scattering and Absorption by Magnetic Materials* (Oxford Science, Oxford, 1996).

¹⁵H. Stragier, J.O. Cross, J.J. Rehr, L.B. Sorensen, C.E. Bouldin, and J.C. Woicik, Phys. Rev. Lett. **69**, 3064 (1992).

¹⁶T.R. Thurston, G. Helgesen, D. Gibbs, J.P. Hill, B.D. Gaulin, and G. Shirane, Phys. Rev. Lett. **70**, 3151 (1993).

¹⁷P.M. Gehring, K. Hirota, C.F. Majkrzak, and G. Shirane, Phys. Rev. Lett. **71**, 1087 (1993).

¹⁸G.M. Watson, B.D. Gaulin, D. Gibbs, T.R. Thurston, P.J. Simpson, S.M. Shapiro, G.H. Lander, H.J. Matzke, S. Wang, and M. Dudley, Phys. Rev. B **53**, 686 (1996).

¹⁹M.P. Zinkin, D.F. McMorrow, J.P. Hill, R.A. Cowley, J.-G. Lussier, A. Gibaud, G. Grübel, and C. Sutter, Phys. Rev. B **54**, 3115 (1996).

²⁰M. Altarelli, M.D. Núñez-Regueiro, and M. Papoular, Phys. Rev. Lett. **74**, 3840 (1995).

²¹V.A. Sidorov, M. Nicklas, P.G. Pagliuso, J.L. Sarrao, Y. Bang, A.V. Balatsky, and J.D. Thompson, Phys. Rev. Lett. **89**, 157004 (2002).

²²A. Bianchi, R. Movshovich, I. Vekhter, P.G. Pagliuso, and J.L. Sarrao, Phys. Rev. Lett. **91**, 257001 (2003).

²³W. Bao, G. Aeppli, J.W. Lynn, P.G. Pagliuso, J.L. Sarrao, M.F. Hundley, J.D. Thompson, and Z. Fisk, Phys. Rev. B **65**, 100505 (2002).